Mechanism of the enhanced conductance of a molecular junction under tensile stress

Alireza Saffarzadeh,[1,2,*] Firuz Demir,[2] and George Kirczenow[2]

[1]*Department of Physics, Payame Noor University, P.O. Box 19395-3697, Tehran, Iran*

[2]*Department of Physics, Simon Fraser University, Burnaby, British Columbia, Canada V5A 1S6*

Despite its fundamental importance for nanophysics and chemistry and potential device applications, the relationship between atomic structure and electronic transport in molecular nanostructures is not well understood. Thus the experimentally observed increase of the conductance of some molecular nanojunctions when they are stretched continues to be counterintuitive and controversial. Here we explore this phenomenon in propanedithiolate molecules bridging gold electrodes by means of *ab initio* computations and semiempirical modeling. We show that in this system it is due to changes in Au-S-C bond angles and strains in the gold electrodes, rather than to the previously proposed mechanisms of Au-S bond stretching and an associated energy shift of the highest occupied molecular orbital and/or Au atomic chain formation. Our findings indicate that conductance enhancement in response to the application of tensile stress should be a generic property of molecular junctions in which the molecule is thiol-bonded in a similar way to gold electrodes.

PACS number(s): 85.65.+h, 81.07.Nb

I. INTRODUCTION

Molecular junctions in which a single molecule forms a stable electrically conducting bridge between two metal electrodes have been studied intensively experimentally and theoretically for more than a decade due to their fundamental interest and potential device applications [1]. Achieving control over the electronic transport properties of these nanostructures is crucial for the realization of practical single-molecule electronic devices. The electronic conductances of molecular junctions are sensitive to their atomic geometries [1]. These geometries can be modified by varying the separation between the two metal electrodes of the molecular junction, and this approach has been used to modulate the conductances of a variety of molecular junctions, including those in which benzenedithiolate (BDT) [2,3], octanedithiolate [4,5], bipyridine [4], or propanedithiolate (PDT) [6] molecules bridge a pair of gold electrodes. In the case of Au-BDT-Au, conductance changes of more than three orders of magnitude have been achieved in this way [3]. Thus BDT has been proposed recently as a candidate for applications as a broad range coherent molecular conductor with tunable conductance [3]. However, despite its great importance for molecular electronics, the present-day understanding of the relationship between the structure and electronic transport characteristics of molecular junctions remains far from complete. For example, intuitively, one might expect the conductance of a molecular junction to decrease as the junction is stretched and the interatomic bonds within it are weakened and therefore become less conducting. However, a recent experiment [2] on Au-BDT-Au junctions has demonstrated that, surprisingly, this need not always be the case, and that, on the contrary, stretching these junctions can result in their conductances *increasing* by more than an order of magnitude. This increase in the conductance was attributed [2] to a strain-induced shift of the highest occupied molecular orbital (HOMO) toward the

Fermi level of the electrodes resulting in resonant tunneling, as was predicted by theories on the dependence of the HOMO energy on the molecule-electrode separation, i.e., the Au-S bond length [7–12]. However, another recent study [3] has indicated that the conductance of Au-BDT-Au junctions is controlled mainly by the strength of the molecule-electrode coupling rather than by the energy of a molecular electronic level. Most recently, it has been proposed [13] that gold atomic chains formed at the molecule-electrode interfaces when the junction is stretched may be responsible for the large increase observed [2] in the conductance. Thus the origin of the observed behavior [2] remains controversial. Interestingly, the conductances of Au-PDT-Au junctions have also been found experimentally to increase as the junctions are stretched at cryogenic temperatures [6]. While the bonding geometries between the molecule and gold electrodes in Au-BDT-Au junctions have not as yet been determined experimentally and remain the subject of conjecture [1], experimental [6] and theoretical [14–16] inelastic tunneling spectroscopy (IETS) studies have determined the experimentally realized molecule-gold bonding geometries in Au-PDT-Au junctions. For this reason, Au-PDT-Au junctions may be more amenable as model systems for developing a *definitive* understanding of the counterintuitive increase of the conductance as the junction is stretched. We therefore explore this phenomenon in Au-PDT-Au junctions theoretically in this article. We present a comprehensive analysis of the relationship between the molecular configuration, contact geometry, and molecular conductance as the junction is stretched. We find the calculated conductance to increase by factors consistent with experiment [6] as the junction is stretched. Before the junction ruptures, we find the conductance to *decrease*, as in the experiment in Ref. [6]. We find the conductance to decrease shortly before and during the formation of a gold atomic chain at a molecule-electrode interface, but the conductance increase resumes with further stretching once an atomic chain has formed. However, we find the conductance increases for junctions with atomic chains to be somewhat smaller than for those without them. We show the increasing conductance as the junction is stretched to be due mainly to increasing

---

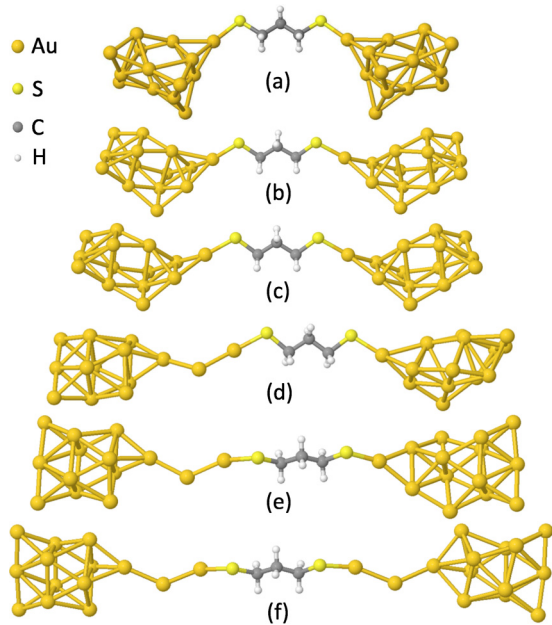*Author to whom all correspondence should be addressed: asaffarz@sfu.ca

FIG. 1. (Color online) Relaxed structures of the Au-PDT-Au molecular junction for various distances d between the outermost atoms of the Au clusters. (a) $d = 21.75$ Å, (b) $d = 25.70$ Å, (c) $d = 26.50$ Å, (d) $d = 29.00$ Å, (e) $d = 30.00$ Å, and (f) $d = 33.40$ Å. As the junction is stretched, Au-Au bonds near the molecule break in succession until in (f) the molecule is connected to each Au cluster by a chain of Au atoms.

Au-S-C bond angles at the molecule-electrode interfaces and strains in the electrodes (geometrical changes that are expected to occur in many molecular junctions under tensile stress) rather than to atomic chain formation or elongation of the Au-S bonds. We find the latter to be too small to affect the measured conductance [6] strongly.

II. ESTIMATION OF THE JUNCTION GEOMETRIES

We study the evolution of the molecular junction's geometry as the Au-PDT-Au junction is stretched by carrying out *ab initio* calculations of the relaxed geometries of extended molecules each consisting of a PDT molecule and two 14-atom gold clusters bound to the PDT sulfur atoms, as shown in Fig. 1. Our previous work [14–16] showed the electronic transport properties of Au-PDT-Au extended molecules to have converged sufficiently with increasing gold cluster size that 14-atom gold clusters can serve as a realistic model of the macroscopic gold electrodes that contact the PDT molecule in experiments [6]. Our starting point is the relaxed geometry shown in Fig. 1(a) that our IETS studies [14–16] identified as having the gold-sulfur bonding geometry that was most commonly realized in experiments [6] on Au-PDT-Au junctions. The other structures that we considered were generated from this one by moving the atom of each gold cluster that was furthest from the molecule slightly further from or closer to the molecule and then freezing the positions of these two outer atoms and relaxing the positions of all of the other atoms of the extended molecule. This procedure was iterated to produce relaxed junction geometries with differing

distances between the two outer Au atoms. Examples are shown in Fig. 1. The relaxations were all carried out using the GAUSSIAN 09 package with the B3PW91 functional and Lanl2DZ pseudopotentials and basis sets [17,18] to locate local minima of the total energy of the extended molecule computed within density functional theory.

Since our approach to calculating the molecular junction geometries is fully quantum mechanical and the total energies of the trial geometries sampled in the relaxation process are computed within density functional theory, our relaxed geometries are expected to be more accurate than those obtained using computationally less demanding methods that employ parametrized interatomic potentials and classical mechanics, such as those in Ref. [13].

Since our geometry relaxations were performed effectively at zero temperature, the relaxed structures that we obtained may be expected to be representative of those realized in the cryogenic temperature experiments of Hihath *et al.* [6] on Au-PDT-Au junctions, especially in view of the fact that our starting molecule-electrode bonding geometry before the junction was stretched was that previously identified as the one most commonly realized in those experiments [14–16]. The fact that the bonding geometry most commonly realized in the experiments on Au-PDT-Au junctions [6] is known [14–16] obviated the need for us to perform relaxations/stretching for a large ensemble of different starting junction geometries such as was necessary in the study in Ref. [13] of Au-BDT-Au junctions, for which the bonding geometry most commonly realized in experiments has yet to be determined.

III. CONDUCTANCE CALCULATIONS

We calculate the zero bias conductance g at the Fermi energy for the Au-PDT-Au molecular wire at various elongations from the Landauer formula [1],

$$g = g_0 \sum_{i,j} |t_{ji}|^2 \frac{v_j}{v_i}, \tag{1}$$

where $g_0 = 2e^2/h$, t_{ji} is the transmission amplitude through the PDT molecule, i is the electronic state of a carrier with velocity v_i that is coming from the left lead, and j is the electronic state of a carrier with velocity v_j that has been transmitted to the right lead. To couple the extended molecule to the electron reservoirs, as in previous work [14–16,19–25], we attach a large number of semi-infinite quasi-one-dimensional ideal leads to the valence orbitals of the outer gold atoms of the extended molecule. We find the transmission amplitudes t_{ji} by solving the Lippmann-Schwinger equation

$$|\Psi^\alpha\rangle = |\Phi_0^\alpha\rangle + G_0(E)W|\Psi^\alpha\rangle, \tag{2}$$

where $|\Phi_0^\alpha\rangle$ is an electron eigenstate of the αth ideal semi-infinite one-dimensional left lead that is decoupled from the extended molecule, $G_0(E)$ is the Green's function of the decoupled system of the ideal leads and the extended molecule, W is the coupling between the extended molecule and the ideal leads, and $|\Psi^\alpha\rangle$ is the scattering eigenstate of the complete coupled system associated with the incident electron state $|\Phi_0^\alpha\rangle$. The semiempirical extended Hückel model [1] with the parameters of Ammeter *et al.* [26] was

used to evaluate the Hamiltonian matrix elements and atomic valence orbital overlaps that enter the Green's function $G_0(E)$ in Eq. (2). As has been discussed in Refs. [1] and [19], this methodology involves no fitting to any experimental data relating to transport in molecular junctions. It is known to yield low bias conductances in reasonably good agreement with experiments for PDT bridging gold electrodes [14,15] as well as other molecules thiol-bonded to gold electrodes [1,19,27–30].

We note that density functional theory (DFT) -based transport calculations are often used to calculate the conductances of molecular junctions [1]. For example, transport calculations based on DFT with approximate self-interaction corrections have been used in the recent theoretical study [13] of the conductance enhancement of Au-BDT-Au junctions under tensile stress. However, density functional theory is a tool designed specifically for calculating ground-state total energies [31,32]. Thus it is appropriate to use DFT to calculate molecular junction geometries, as is done in the present work, since these geometries are found by minimizing the total energy. On the other hand, transport is *not* a ground-state property. For this reason, DFT-based transport calculations are not well justified at the fundamental level, and the results obtained from them in practice are often unreliable [1]. Attempts are being made to correct for these limitations of DFT [1], however these corrections involve uncontrolled approximations and their effectiveness is uncertain at this time. Moreover, DFT-based transport calculations are especially problematic for the case in which the distances between the molecule and the contacts in a molecular junction are being varied, as has been discussed by Koentopp *et al.* [33] and others [1]. For these reasons, it is unclear whether any counterintuitive transport effect predicted by a DFT-based theory in a molecular junction under tensile strain is physical or an artifact of the shortcomings of DFT and/or any corrections that have been applied to it. We therefore prefer to use instead the semiempirical extended Hückel theory-based approach to transport that has been outlined and justified in the preceding paragraph.

IV. RESULTS

The calculated conductances of our relaxed structures are plotted in Fig. 2 versus the junction length d, i.e., the distance d between the outermost atoms of the two gold clusters. The structure in Fig. 1(a) (with $d = 21.75$ Å and labeled U in Fig. 2) is an unstrained junction since it was relaxed without constraints on any atoms.

Figure 2 shows that when a compressive strain is applied to the unstrained junction, the conductance of the junction decreases (red circles to the left of U in Fig. 2). A larger drop in the conductance occurs when the molecular geometry switches from trans (red circles) to gauche (blue circles) under compressive strain. Lower conductances for gauche than trans conformations of other molecular wires have been predicted previously [34,35]. Note that, in the present work, gauche conformations (blue circles) were formed only for $d \leqslant 21.10$ Å; for all other junction lengths, only trans molecular conformations were found.

On the other hand, stretching the junction from $d = 21.75$ Å (U in Fig. 2) to $d = 29.50$ Å results in an increasing junction
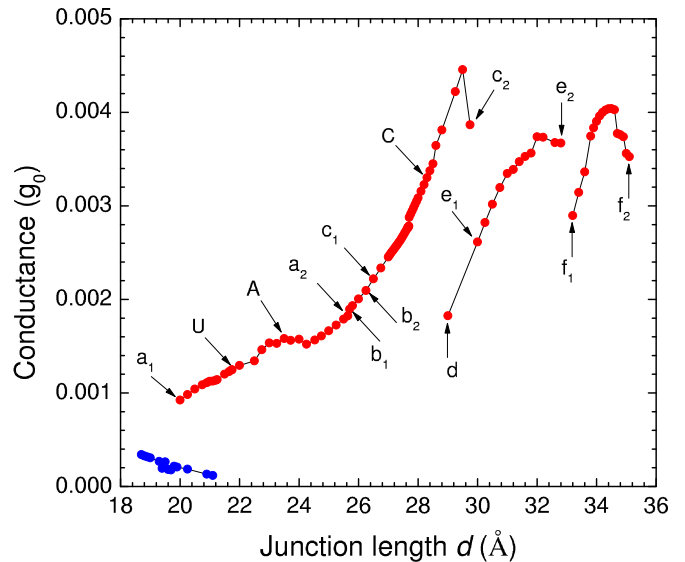

FIG. 2. (Color online) Calculated conductance at zero temperature of trans (gauche) Au-PDT-Au junctions vs junction length for different structures is shown in red (blue). Red circles between a_1 and a_2, b_1 and b_2, c_1 and c_2, e_1 and e_2, and between f_1 and f_2 show the conductances for structures similar to Figs. 1(a), 1(b), 1(c), 1(e), and 1(f), respectively. Point d indicates the structure shown in Fig. 1(d). A and C are explained in the inset of Fig. 3. U is the unstrained junction.

conductance followed by a decrease at $d = 29.75$ Å (labeled c_2 in Fig. 2) which signals that the junction is close to rupturing or forming an Au atomic chain as in Fig. 1(e). In the junction length interval from $d = 20.00$ to 25.64 Å, i.e., from a_1 to a_2 in Fig. 2, the nearest gold atoms to the PDT molecule bond to three neighboring gold atoms, and the junction geometry for the trans molecular conformation stays qualitatively similar to that in Fig. 1(a). At $d = 25.70$ Å, labeled b_1 in Fig. 2, a bond breaks between the Au atom at the tip of the right gold cluster and one of its neighbors, as shown in Fig. 1(b). However, interestingly, this bond breaking does not result in any drop in the conductance, which, on the contrary, continues to rise. The nature of the resulting bonding geometry is maintained until $d = 26.25$ Å, labeled b_2. At $d = 26.50$ Å labeled c_1 a bond breaks between the Au atom at the tip of the left cluster and one of its neighbors, resulting in a structure similar to that in Fig. 1(c). However, the conductance continues to rise smoothly as the junction is stretched, although with an increasing slope until $d = 29.75$ Å (c_2), where the conductance declines although the structure remains qualitatively similar to that in Fig. 1(c).

We find further stretching to result in either rupture of the junction or formation of a chain of gold atoms between the molecule and one of the gold clusters, depending on the details of the stretching procedure. Formation of the atomic chain results in the structure shown in Fig. 1(e) and a significant drop in the conductance to the value labeled e_1 in Fig. 2. This conductance drop is reasonable because gold atomic chains have only a single conducting quantum channel as compared to the multiple channels in the gold clusters. Compressing the structure in Fig. 1(e) results in the structure in Fig. 1(d) and

a decline in the junction conductance from e_1 to d in Fig. 2. Interestingly, although the structure in Fig. 1(d) involves a gold atomic chain, its junction length $d = 29.00$ Å is smaller than that of c_2 ($d = 29.75$ Å), although the latter structure has no atomic chain and resembles Fig. 1(c). If the junction in Fig. 1(d) or Fig. 1(e) is stretched, the conductance resumes its increase until the junction length approaches $d = 32.80$ at e_2 in Fig. 2, where a small decrease in the conductance again heralds the appearance of a Au atomic chain, this time at the right Au cluster [Fig. 1(f)]. The formation of this chain with $d = 33.00$ Å again results in an abrupt drop in the conductance to the value labeled f_1 in Fig. 2. Thus an abrupt drop in conductance when an Au atomic chain is formed appears to be a generic property of this system. Upon further stretching of the junction from $d = 33.00$ to 35.10 Å, i.e., from f_1 to f_2, the conductance increases and then declines while the number of Au-Au bonds between the tips of the gold clusters and the adjacent gold atoms remains the same; the elongation of the junction results in changes in various bond angles in the system.

Our numerical results show that the responses of the electronic energy eigenvalues and eigenvectors of the extended molecule to stretching of the junction both contribute to the rises in the conductance. The details are complex since several pairs of almost degenerate eigenstates mediate conduction through the molecule, and the contributions of the two states of each degenerate pair interfere destructively with each other. The reason for the destructive interference is that the two degenerate states have opposite parity (within the PDT molecule) with respect to the approximate left-right mirror symmetry of the PDT molecules in Fig. 1.

However, we shall show that the physics underlying conductance increases as the junction is stretched can be identified by examining the relationship between the conductance and the geometrical changes that occur in the junction. Stretching results in changes in the chemical bond lengths and bond angles in the junction. For example, when the junction length increases from $d = 29.00$ to 32.80 Å (i.e., from d to e_2 in Fig. 2), the S-Au bond lengths increase by only a small amount (0.05 Å), while the C-S-Au bond angles at the left (right) end of the molecule change from 110.15° to 118.60° (108.07° to 119.40°), indicating that most of the elongation is due to changes in bond angles. Importantly, during this elongation the conductance of the junction increases by a factor of ∼2, but we find that only a small ∼16% conductance change can be attributed to the elongation of the Au-S bonds. We find that much greater elongation of the Au-S bonds (by 0.6 Å) would result in large conductance increases (by factors ∼4) due to a transport resonance approaching the electrode Fermi level, qualitatively similar to the findings of previous theories relating the conductance of Au-BDT-Au junctions to the molecule-electrode separation [7–12]. However, our *ab initio* junction geometry calculations show such large Au-S bond elongations to be an order of magnitude larger than those predicted to be realized during the experimental conductance measurements [6], and therefore not relevant to the observed conductance increases.

Thus we turn now to the role of the bond angles in the conductance. Figure 3 shows the dependence on the junction length d of the C-S-Au angles, and also the S-Au-Au and
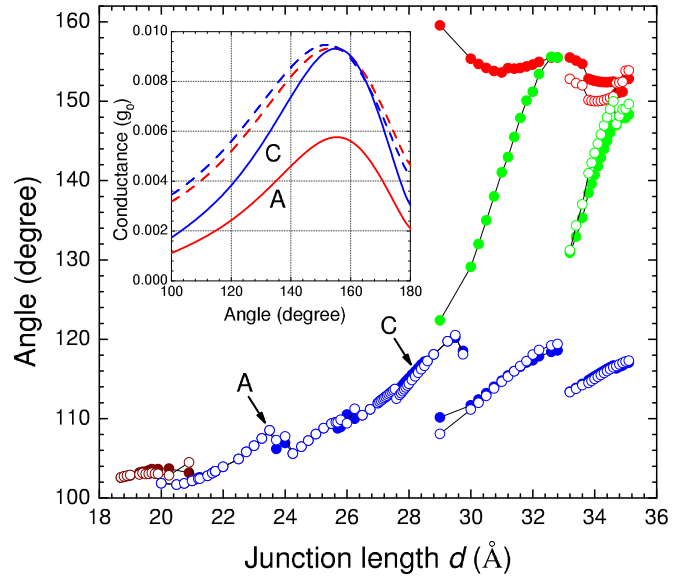

FIG. 3. (Color online) Variation of the C-S-Au (blue), S-Au-Au (red), and Au-Au-Au (green) angles for trans-PDT junctions with junction length d. C-S-Au angles for gauche structures are maroon. Solid (hollow) circles show angles to the left (right) of the molecule. The solid (dashed) lines in the inset show the conductance vs C-S-Au angle for junctions obtained from those marked A and C in Figs. 2 and 3 by rigidly rotating the 14 (1) -atom gold clusters about the S atoms.

Au-Au-Au angles when an Au atomic chain forms. The corresponding angles at the left and right ends of the molecule (solid and hollow circles) are very similar. The dependence of the C-S-Au bond angles (blue circles) in Fig. 3 on the junction length d is strikingly similar to that of the conductance in Fig. 2; the main features of either plot are reproduced in the other almost quantitatively. In contrast, although the S-Au-Au and Au-Au-Au angles depend on d and the latter angle even changes by more than 30° in the stretching process, the role of these angles is not crucial in the conductance increase, since conduction through Au atoms is mainly via the isotropic s orbitals.

To better understand the role of the bond angles, we chose two junctions marked A and C in Figs. 2 and 3. For these we computed the dependence of the conductance on the C-S-Au angles *alone*, varying these angles by rotating the gold clusters rigidly about the S atoms, holding the PDT molecule fixed. This yielded the solid curves in the inset of Fig. 3. These plots show that for each structure A or C, the dependence of the conductance on the C-S-Au angles accounts for roughly half of the conductance change between a_1 and c_2 in Fig. 2, the remainder being due mainly to the structural differences between the A and C gold clusters. A similar calculation but including only one Au atom from each Au cluster yielded the dashed curves in the inset of Fig. 3. Since the difference between the dashed red and blue curves is small and is due to the stretching of the Au-S bonds and structural changes within the PDT molecule itself in going between structures A and C, we conclude that these effects make at most minor contributions to the conductance increase when the junction is stretched.

As has been discussed above, we find the conductances of Au-PDT-Au junctions to increase by similar amounts as the junction is stretched, whether a gold atomic chain is present at the interface between the molecule and one of the gold electrodes, or at the interfaces between the molecule and both of the gold electrodes, or at neither interface. However, the maximal value of this conductance increase is somewhat larger if there is no gold atomic chain present than in either of the latter two cases. In contrast, in Ref. [13] it has been predicted that for Au-BDT-Au junctions the conductance increase in response to stretching of the junction is much larger if a gold atomic chain forms than if it does not. The mechanism proposed in Ref. [13] for this very large conductance increase is unrelated to the mechanism of conductance enhancement in Au-PDT-Au junctions that we propose in the present article. The conductance increase predicted in Ref. [13] is due to a strong feature in the Au s and p density of states of the atomic chains near the Fermi energy that results in enhanced electron transmission through the molecular junction. Some caution regarding this prediction is in order since it is the result of DFT-based transport calculations, although a self-interaction correction intended to address some of the deficiencies of DFT was included in the calculation [13].

V. CONCLUSIONS

In summary, we have presented a systematic exploration of the response of the conductance of propanedithiolate molecular nanowires bridging gold electrodes to mechanical stretching of this junction, based on *ab initio* density functional theory and semiempirical techniques. Our results demonstrate theoretically that the counterintuitive phenomenon of increasing conductance in response to junction elongation should occur in a gold-alkanedithiolate-gold junction. We showed that three different junction geometries can each show a

conductance increase in response to junction elongation followed by a conductance decrease and either rupture or a transition to a different junction geometry. A very similar conductance increase followed by a decrease and subsequent junction rupture has been observed experimentally in an Au-PDT-Au junction and can be seen in Fig. 4(a) of Ref. [6]. We showed the conductance increases to be due primarily to increases in the C-S-Au bond angles at the molecule-electrode interfaces and to atomic rearrangements in the gold electrodes. Conductance increases in response to increasing C-S-Au bond angles are reasonable because of the important role that carbon and sulfur atomic valence p-orbitals play in transport through organic molecules and the anisotropic nature of the overlaps between these orbitals on different atoms. For this reason, we expect the mechanism of the conductance increase under tensile stress that we have identified to be active in all molecular junctions with molecules thiol bonded in a similar way to gold electrodes. Therefore, we predict that this interesting phenomenon is a universal generic property of such junctions. We have also demonstrated that changes in the Au-S bond length and in the structure of the propanedithiolate molecule that occur in response to elongation of the junction play a minor role in the observed conductance increase. Our findings also demonstrate that electron transport through the PDT molecule can be controlled by varying the length of the junction and that both continuous modulation of the conductance and abrupt switching between high and low conductance states can be induced in this way. These remarkable changes in the molecular conductance indicate that alkanedithiol molecular nanowires have potential applications as mechanical switches in nanoscale devices.

ACKNOWLEDGMENTS

[1] For a recent review, see G. Kirczenow, in *The Oxford Handbook of Nanoscience and Technology, Volume I: Basic Aspects*, edited by A. V. Narlikar and Y. Y. Fu (Oxford University Press, Oxford, 2010), Chap. 4.

[2] C. Bruot, J. Hihath, and N. Tao, Nat. Nanotechnol. **7**, 35 (2012).

[3] Y. Kim, T. Pietsch, A. Erbe, W. Belzig, and E. Scheer, Nano Lett. **11**, 3734 (2011).

[4] B. Xu, X. Xiao, and N. J. Tao, J. Am. Chem. Soc. **125**, 16164 (2003).

[5] Z. Huang, F. Chen, P. A. Bennett, and N. Tao, J. Am. Chem. Soc. **129**, 13225 (2007).

[6] J. Hihath, C. R. Arroyo, G. Rubio-Bollinger, N. Tao, and N. Agraït, Nano. Lett. **8**, 1673 (2008).

[7] D. Q. Andrews, R. Cohen, R. P. van Duyne, and M. A. Ratner, J. Chem. Phys. **125**, 174718 (2006).

[8] S. H. Ke, H. U. Baranger, and W. Yang, J. Chem. Phys. **122**, 074704 (2005).

[9] L. Romaner, G. Heimel, M. Gruber, J. L. Brédas, and E. Zojer, Small **2**, 1468 (2006).

[10] Z. Li and D. S. Kosov, Phys. Rev. B **76**, 035415 (2007).

[11] C. Toher and S. Sanvito, Phys. Rev. Lett. **99**, 056801 (2007).

[12] R. B. Pontes, A. R. Rocha, S. Sanvito, A. Fazzio, and A. J. Roque da Silva, ACS Nano **5**, 795 (2011).

[13] W. R. French, C. R. Iacovella, I. Rungger, A. M. Souza, S. Sanvito, and P. T. Cummings, Nanoscale **5**, 3654 (2013).

[14] F. Demir and G. Kirczenow, J. Chem. Phys. **134**, 121103 (2011).

[15] F. Demir and G. Kirczenow, J. Chem. Phys. **136**, 014703 (2012).

[16] F. Demir and G. Kirczenow, J. Chem. Phys. **137**, 094703 (2012).

[17] M. J. Frisch, G. W. Trucks, H. B. Schlegel, G. E. Scuseria, M. A. Robb, J. R. Cheeseman, G. Scalmani, V. Barone, B. Mennucci, G. A. Petersson *et al*., the GAUSSIAN 09 Revision: A.02 computer code was used.

[18] J. P. Perdew, K. Burke, and M. Ernzerhof, Phys. Rev. Lett. **77**, 3865 (1996).

[19] D. M. Cardamone and G. Kirczenow, Phys. Rev. B **77**, 165403 (2008); Nano Lett. **10**, 1158 (2010).

[20] G. Kirczenow, P. G. Piva, and R. A. Wolkow, Phys. Rev. B **72**, 245306 (2005); **80**, 035309 (2009).

[21] P. G. Piva, R. A. Wolkow, and G. Kirczenow, Phys. Rev. Lett. **101**, 106801 (2008).

[22] H. Dalgleish and G. Kirczenow, Phys. Rev. B **72**, 155429 (2005); Nano Lett. **6**, 1274 (2006).

[23] G. Kirczenow, Phys. Rev. B **75**, 045428 (2007).

[24] F. R. Renani and G. Kirczenow, Phys. Rev. B **84**, 180408(R) (2011); **85**, 245415 (2012); **87**, 121403(R) (2013).

[25] A. Saffarzadeh and G. Kirczenow, Appl. Phys. Lett. **102**, 173101 (2013).

[26] The version of extended Hückel theory used was that of J. H. Ammeter, H.-B. Bürgi, J. C. Thibeault, and R. Hoffman, J. Am. Chem. Soc. **100**, 3686 (1978); as implemented in the YAEHMOP numerical package by G. A. Landrum and W. V. Glassey (Source-Forge, Fremont, CA, 2001).

[27] J. G. Kushmerick, D. B. Holt, J. C. Yang, J. Naciri, M. H. Moore, and R. Shashidhar, Phys. Rev. Lett. **89**, 086802 (2002).

[28] S. Datta, W. D. Tian, S. H. Hong, R. Reifenberger, J. I. Henderson, and C. P. Kubiak, Phys. Rev. Lett. **79**, 2530 (1997).

[29] E. G. Emberly and G. Kirczenow, Phys. Rev. Lett. **87**, 269701 (2001).

[30] E. G. Emberly and G. Kirczenow, Phys. Rev. B **64**, 235412 (2001).

[31] P. Hohenberg and W. Kohn, Phys. Rev. **136**, B864 (1964).

[32] W. Kohn and L. J. Sham, Phys. Rev. **140**, A1133 (1965).

[33] M. Koentopp, C. Chang, K. Burke, and R. Car, J. Phys.: Condens. Matter **20**, 083203 (2008).

[34] C. Li, I. Pobelov, T. Wandlowski, A. Bagrets, A. Arnold, and F. Evers, J. Am. Chem. Soc. **130**, 318 (2008).

[35] M. Paulsson, C. Krag, T. Frederiksen, and M. Brandbyge, Nano Lett. **9**, 117 (2009).